17th World Conference on Earthquake Engineering, 17WCEE
Sendai, Japan - September 13th to 18th 2020

PLANAR AND SPATIAL INVESTIGATION OF EARTHQUAKE INDUCED POUNDING OF BASE ISOLATED BUILDINGS

P. Komodromos[(1)], E. Mavronicola[(2)], P. Polycarpou[(3)]

[(1)] *Associate Professor, University of Cyprus, komodromos@ucy.ac.cy*
[(2)] *Research Associate, University of Cyprus, mavronicola.eftychia@ucy.ac.cy*
[(3)] *Assistant Professor, University of Nicosia, polycarpou.p@unic.ac.cy*

Abstract

Seismic isolation is utilized in relatively stiff buildings to avoid resonance with the predominant frequencies of typical seismic excitations and reduce the induced seismic loads, floor accelerations and interstory drifts, while large strains are confined at the isolation level. Although a wide seismic gap is provided around a base isolated building (BIB) to accommodate the expected large relative displacements at the isolation level, since its width is often finite, there is a possibility of pounding with the surrounding moat wall or adjacent structures during a stronger than expected earthquake excitation. This research work investigates, through both planar and spatial simulations, that possibility and assesses how potential structural pounding may affect the effectiveness of seismic isolation.

Conducted planar analyses reveal that the peak interstory drifts ratio of a BIB increases significantly due to structural impact with the adjacent moat wall, reaching values that are several times the corresponding peak response values without pounding, and that such an increase is, in general, amplified as the width of the seismic gap between the BIB and the adjoining moat wall reduces.

Subsequently, three-dimensional (3D) analyses are used to take into account other spatial factors, such as the incidence angle of the imposed seismic excitations, potential mass eccentricities and torsional effects, which cannot be considered through planar simulations. Multi-degree-of-freedom (DOF) systems of 3 dynamic DOF at each floor level, representing base isolated buildings, with impact capabilities, subjected to two orthogonal seismic components, of which the incidence angle may vary are simulated using a specially designed 3D software. The developed software enables the spatial simulation of buildings modeled as 3D MDOF systems with shear-type behavior, while the nonlinear inelastic bidirectional coupled Bouc–Wen model is employed for simulating the isolation system, which is assumed to consist of lead rubber bearings (LRBs). The software enables the consideration of pounding with both the surrounding moat wall and adjacent conventionally fixed-supported buildings.

The conducted spatial simulations show that the critical angle of incidence differs, depending on the characteristics of the imposed seismic excitations. Thus, the customary practice of imposing the earthquake excitations along the major construction axes of the BIB may lead to significant underestimations of the peak structural response in case of pounding during strong earthquake excitations. Moreover, the seismic incidence angle influences significantly the width of the required seismic gap that should be provided as clearance to avoid structural impact. In addition, the effect of the directionality of the imposed seismic ground motions, as well as the number of floors and the fundamental eigenperiod of the adjacent structures, influence the possibility of structural pounding and the severity of the peak structural response in case of impact during severe seismic excitations.

Keywords: base/seismic isolation; structural impact; structural pounding; incidence angle; accidental eccentricities

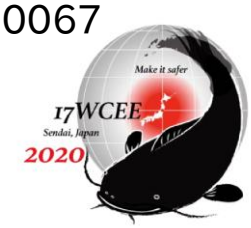

1. Introduction

Although advances in earthquake resistant design have significantly reduced human casualties during strong earthquakes, damage is often unavoidable. The limitation of conventional earthquake-resistance design to avert damage has inspired the usage of innovate passive and active control approaches, such as seismic isolation. Specifically, seismic isolation can be utilized to shift the fundamental eigenperiods of relatively stiff buildings outside the dangerous for resonance range, in order to reduce the induced seismic loads and prevent the disastrous consequences of severe earthquake excitations. The elongation of the fundamental eigenperiod of a building, in order to avoid resonance, is achieved by incorporating flexibility, in the form of seismic isolators, which are usually installed at the base of the building. Essentially, the superstructure of a base isolated building is oscillating like a rigid body, while the interstory deflections and the absolute floor accelerations are significantly decreased so that potential damage of structural and non-structural components, as well as contents of the building, can be averted [1–4].

Although lateral deformations are confined at the seismic isolation level, an energy dissipation mechanism should be provided at the isolation level and a sufficiently wide clearance must be ensured around the building in order to avoid potential structural pounding with adjacent structures during strong earthquakes [5–8] due to the anticipated large relative displacements at the isolation level. Substantial research work of structural pounding has been carried out throughout the last decades on conventionally fixed-supported buildings [9–11] and BIBs [5, 6, 20, 12–19]. However, most of research studies on structural impacts approach the problem in two-dimensions (2D), circumventing the complexities associated with the spatial nature of the problem. A limited number of research works extent the simulation in the more representative and realistic 3D domain [21–29], using spatial nonlinear time-history analyses.

Although some basic effects of structural pounding can be considered using 2D simulations, factors that are directly related to the spatial movement of the structures, cannot be considered in such simulations. Specifically, both orthogonal seismic components of the excitation in the case of 3D simulations may affect the overall response of the building, compared to the corresponding unidirectional excitation that is used in the 2D. Furthermore, in planar simulations involving structural pounding, the impacts are assumed to be normal, ignoring tangential forces that may develop due to friction. The presented research work, which evolved from planar to spatial simulations and parametric studies, aims to understand how structural pounding may affect the effectiveness of seismic isolation and properly assess the required clearance to avoid pounding incidences.

2. Planar (2D) numerical simulations

2.1 Modeling assumptions

This section presents some indicative results from the planar (2D) dynamic analyses of a BIB considering potential structural pounding with the surrounding moat wall. The superstructure of the building is modeled as a shear-type structure isolated with LRBs with one lateral DOF at each floor and the masses lumped at the floor levels, while it is assumed that the superstructure exhibits a linear elastic behavior under the induced seismic excitations. In the presented simulations, pounding might occur only between the moat wall and the base floor when the available clearance is exceeded by the relative displacements at the isolation level.

Specifically, a 3-story BIB with 340 tons lumped masses at the base isolation and at each floor level except the roof which has a mass of 250 tons, which may pound against the adjacent moat wall, is used in the conducted analyses, as shown in Fig. 1(a). Each story has a horizontal stiffness of 600 MN/m, whereas classical Rayleigh damping is employed, assuming viscous damping ratios of 5 % and to 2 % for the fundamental and the last eigenmodes, in addition to the hysteretic energy dissipation due to the nonlinear inelastic behavior of the LRBs at the isolation level. In particular, a smooth bilinear inelastic behavior, according to the Bouc-Wen model, is used to simulate the base isolation system, Fig. 1(b), with an isolation eigenperiod based on the post-yield stiffness of 2.0 s, normalized characteristic strength F_{yi}/W_{tot} = 5% and yield displacement equal to 1.0 cm. For all performed dynamic analyses, the values of 1.0, 0.5, 0.5 and 2 are adopted for the Bouc-Wen [31, 32] models' parameters A, β, γ and n, respectively.

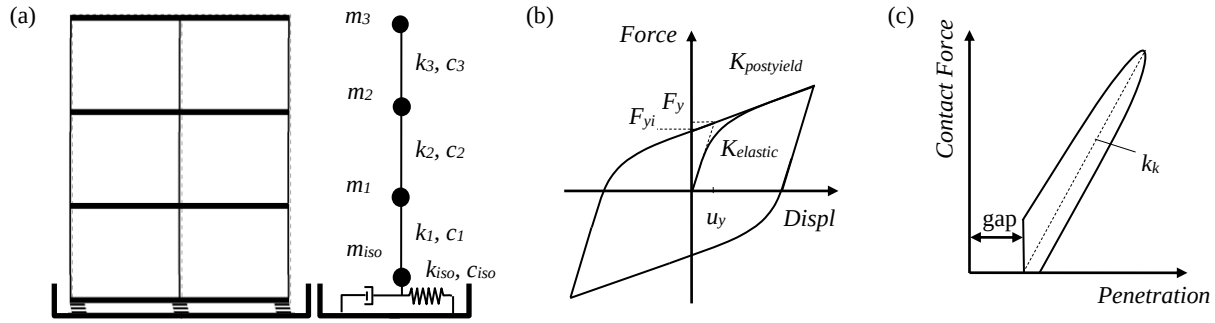

Fig. 1: (a) Configuration of a 3-story BIB, and (b) smooth bilinear inelastic model for the behavior of the seismic isolation system, and (c) modified Kelvin-Voigt element [13].

The modified force-based viscoelastic impact model [13] with impact stiffness of 2,500 kN/mm, is used to take into account structural impact incidences, Fig. 1(c). The coefficient of restitution is assumed to be equal to 0.7 for all cases, while the mass of the surrounding moat wall is set to 500 tons. The fault- normal component (FN Comp) of 5 near-fault ground motions (Table 1) from the Pacific Earthquake Engineering Research Center Database [30], are used in the simulations of this section, in order to examine the effects of the characteristics of the imposed earthquake excitations on the peak seismic response of the BIB during collisions in 2D.

Table 1 – Details of the ground accelerations used in this research work.

Seismic event (Station), Date	Mw	FN Comp			FP Comp		
		PGA (g)	PGV (cm/s)	PGD (cm)	PGA (g)	PGV (cm/s)	PGD (cm)
Loma Prieta (LGPC), 1989	6.93	0.94	97	62.5	0.54	72.1	30.5
Erzican (Erzincan), 1992	6.69	0.49	95.4	32.1	0.42	45.3	16.5
Northridge-01 (Newhall–W Pico Canyon), 1994	6.69	0.43	87.7	55.1	0.28	74.7	21.8
Northridge-01 (Sylmar – Converter), 1994	6.69	0.59	130.3	54	0.8	93.3	53.3
Denali (TAPS Pump Station #10), 2002	7.9	0.33	95.5	92.4	0.27	121.3	116.2

2.2 Influence of the gap size and the characteristics of the earthquake excitation

In this planar parametric study, the seismic gap width, between the BIB and the surrounding moat wall, is varied between 15 and 45 cm with a step of 0.2 cm, in order to investigate its effect on the overall peak seismic responses. The 3-story base-isolated building, with moat wall on both sides of the building, is analyzed under the selected near-fault ground motions. Fig. 2 presents the peak interstory drifts of the BIB in terms of the width of the seismic gap, which show that the most severe response occurs at the base level where poundings occur, i.e. at the 1–0 interface.

The simulation results indicate that the peak interstory drifts ratio of the BIB increases significantly due to structural impact, reaching values that are several times the corresponding peak response values without pounding. It is also observed that the peak seismic response, in terms of interstory drifts, is, in general, amplified as the seismic gap reduces. The amplification of the interstory deflections due to structural poundings reaches values higher than 10 for a seismic gap of 15 cm (for all the excitations except Denali, 2002). Thus, as the seismic gap increases, the interstory drift ratios of the superstructure significantly decrease.

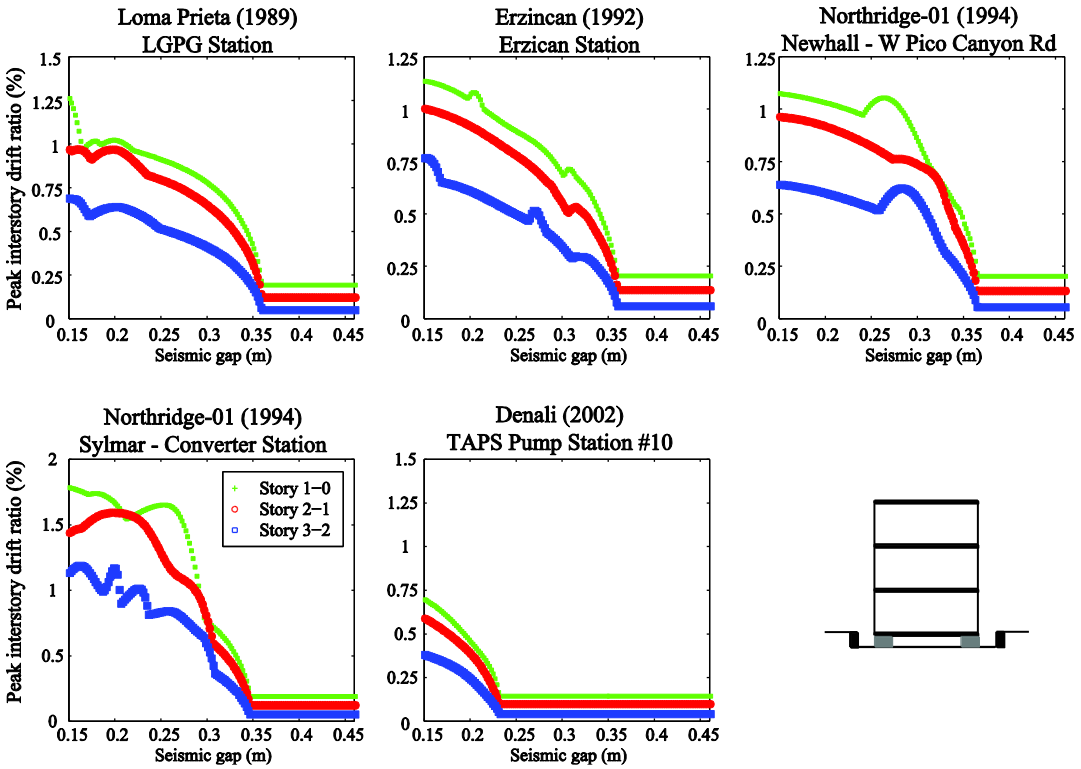

Fig. 2: Peak interstory drift ratios of the 3-story BIB due to poundings with the moat wall in terms of the width of the seismic gap.

3. Spatial (3D) simulations

Performing 3D simulations enables the investigation of certain parameters that are associated with the spatial movement of a BIB and cannot be explored through planar (2D) dynamic analyses. Specifically, the effects of seismic pounding on the peak seismic response of BIBs under bidirectional excitations are investigated, considering a 3D model of a BIB, which takes into account the arbitrary location of impacts and the geometry at the point of impact without any need for an a priori determination of the contact points. The simulated BIBs are modeled as a 3D multi-DOF system with shear-type behavior, for its superstructure, in the horizontal directions. The slab, at each floor level of the superstructure, is represented by a rigid diaphragm that is mathematically simulated as a convex polygon, while the masses are considered to be lumped at the floor levels, having 3 DOFs, i.e. two translational, parallel to the horizontal global axes, and one rotational along the vertical axis. Consequently, it is assumed that the impact forces occur only in horizontal planes.

At each time-step during the imposed seismic excitations, the relative displacements, velocities and absolute accelerations are computed at each dynamic DOF. Based on the deformed position of each floor diaphragm in the 3D space, an automatic contact detection check is performed to identify potential contacts between adjacent structures, which are subsequently used for the computation of the impact forces to be applied at the corresponding DOFs for the next time step.

The majority of the force-based impact models that are available in the scientific literature calculate the impact force as a function of the interpenetration depth between the colliding bodies. However, the usage of the interpenetration depth as the key variable constitutes a significant drawback in the case of 3D impact modelling, as it cannot correctly assess the proper values of the impact forces. In the employed methodology, the area of the overlapping region, instead of the interpenetration depth, is employed as the key variable in the estimation of the impact forces. Further details about the methodology can be found in Polycarpou *et al.* [28].

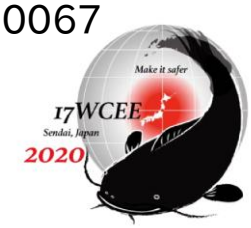

3.1 Data analysis

The peak seismic response of a 3-story reinforced concrete BIB (Fig.4), with 3 x 3 bays of 5.5 m in each direction and 3.2 m high columns with 45 x 45 cm^2 cross sections, has been studied. The modulus of elasticity and the Poisson's ratio are assumed to equal 30 GPa and 0.2, respectively. A 250 tons lumped mass is assumed at the top-floor and a 340 tons lumped mass is considered at each of the other floor levels, as well as at the base of the BIB. The mass distribution is spatially symmetric with respect to the center of gravity, unless otherwise stated. Identical LRBs are used under each of the 16 columns of the BIB, having the same stiffness and damping properties in the two primary directions, with the characteristics given in Fig. 3(b) for each seismic isolator. For the estimation of an equivalent viscous damping matrix, Rayleigh damping is adopted, setting the damping ratios for the fundamental and the last eigenfrequencies to 5% and 2%, respectively, while the hysteretic energy dissipation is directly taken into account by the nonlinear inelastic behavior, according to the Bouc-Wen model, of the seismic isolation system.

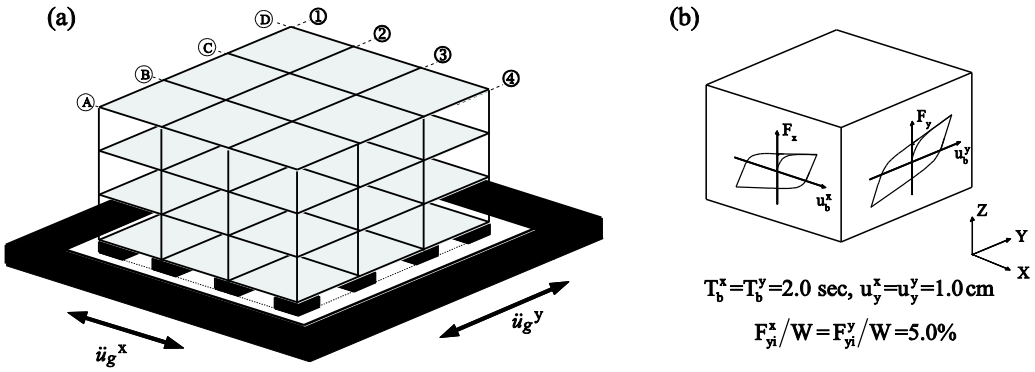

Fig. 3 – Configuration of the BIB considered in the presented research study.

The retaining moat wall, which is assumed to be 100 cm thick and 100 cm high, is modeled considering 3 dynamic DOF with a single mass, considering the two horizontal translations and the rotation around the vertical axis. The mass of the moat wall is assumed to be 5 tons/m, in order to take into account the contribution of the backfill soil. The values of $2.58 \cdot 10^7$ KN/m^2 and $5.74 \cdot 10^6$ KN/m are considered for the impact stiffness in the normal and the tangential directions, respectively, which are typical values for normal strength concrete [28]. Regarding static and kinetic friction, the values of $\mu_s = 0.8$ and $\mu_k = 0.6$, for the respective coefficients, are considered, while a 0.65 coefficient of restitution is adopted, as it has been used in many other relevant studies involving concrete structures [33, 34]. Numerous time-history analyses are performed using the 5 pairs of orthogonal components of recorded horizontal ground-motions, given in Table 1.

3.2 Effect of incidence angle

In order to study the influence of the incidence angle of the imposed ground motion accelerations on the resulting peak seismic response, the two horizontal components of ground acceleration are rotated, with respect to the major construction axes, and resolved along the structural degrees of freedom [35, 36]. Figs. 4 and 5 provide the corresponding peak interstory drift ratios at each floor of the 3-story BIB among its corner columns in terms of the available seismic gap width, for an angle of incidence set equal to 0° and 60°, respectively, for each of the 5 selected seismic excitations. Consistent with the findings of 2D simulations, as the separation distance from the moat wall increases the amplifying effects resulting from poundings decrease.

The computed results indicate that the proximity of the adjacent moat wall to the BIB in combination with the excitation characteristics affect the peak seismic response of the BIB during impact, with the highest peak response exhibited at the base of the building next to the moat wall. It is, also, observed that the critical gap size that is required in order to avoid pounding may vary for different angles of incidence.

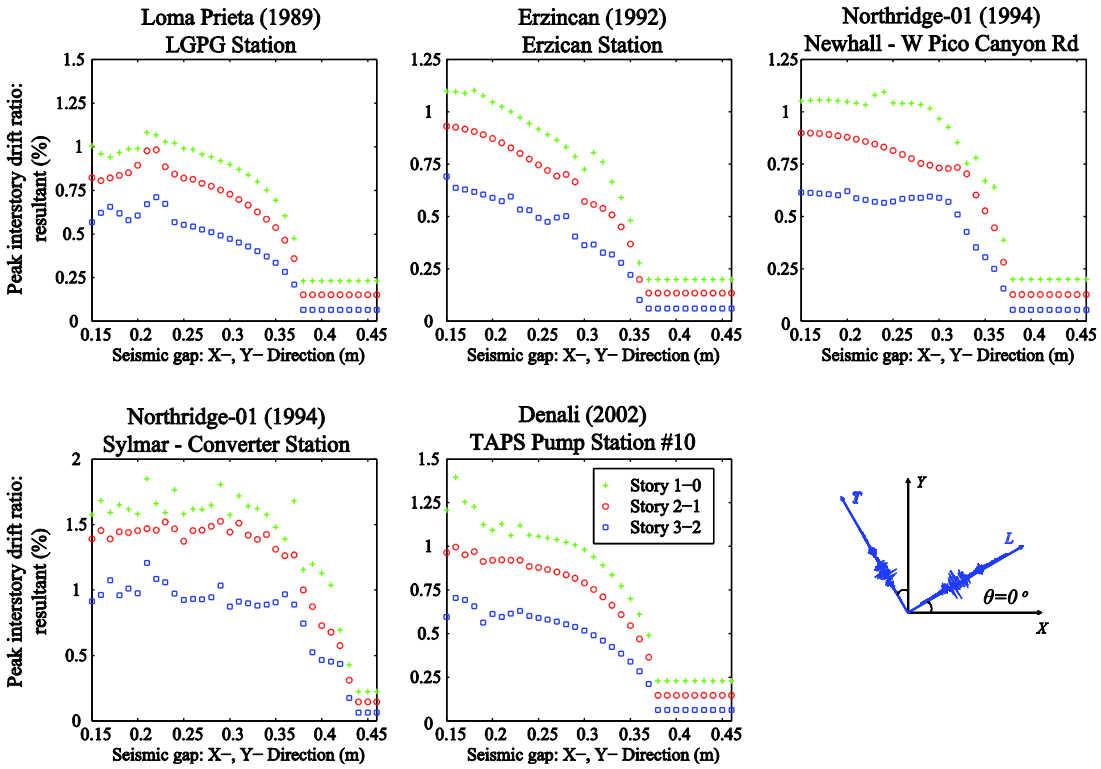

Fig. 4 – Peak responses at each floor of the 3-story BIB among corner columns in terms of the available gap size and a fixed angle of incidence set at 0°.

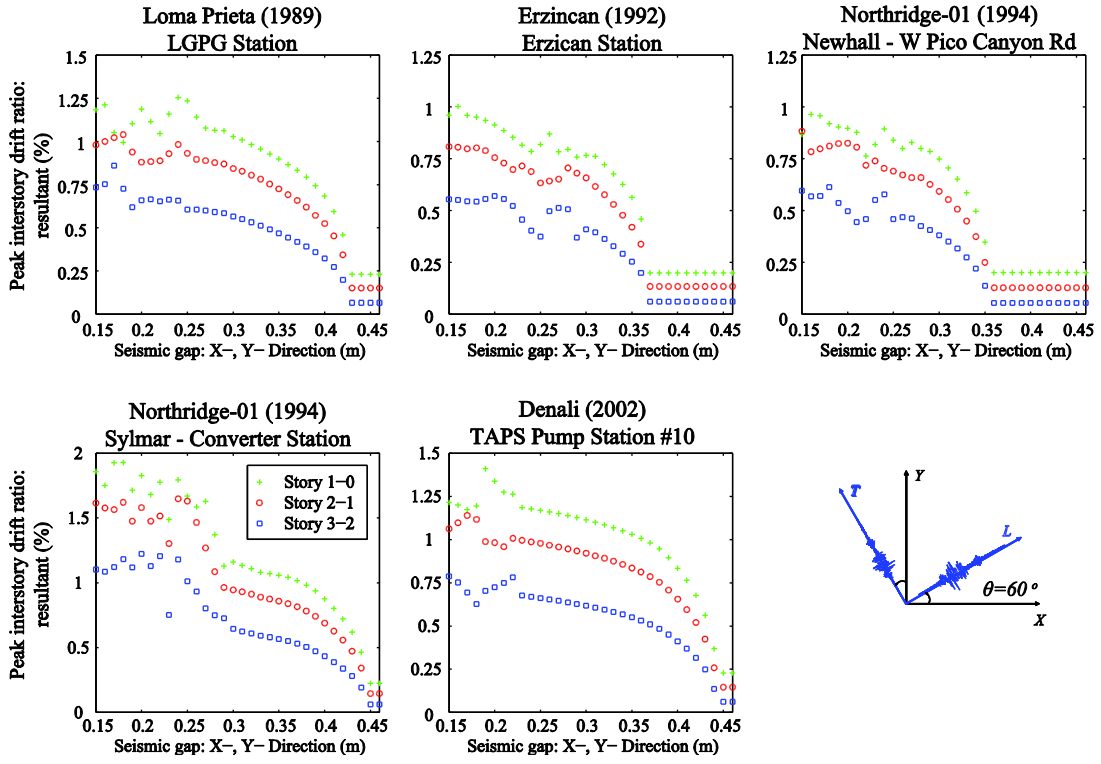

Fig. 5 – Peak responses at each floor of the 3-story BIB among corner columns in terms of the available gap size and a fixed angle of incidence set at 60°.

Next, each of the 5 seismic record pairs, is rotated from 0° to 360°, with respect to the system's principle axes of construction, with a 5° interval in the clockwise direction. The envelopes of the peak interstory drift ratios of the corner column A_1, over all stories of the structure, are provided in Fig. 6, for various seismic incidence angles. Each subplot corresponds to the peak seismic response of a particular excitation, while the gap size around the building is kept at 20 cm. According to the computed results, for each seismic excitation, the peak interstory drift ratio seems to be polarized in the direction along which the peak unobstructed base relative displacement is observed, while the occurrence of impacts generates a significant response dependency on the incidence angle of the imposed seismic excitation. As a consequence, the consideration of the directionality of planar ground motions becomes an essential parameter that should be investigated during the design process. It is apparent that the most severe peak interstory deflections arise at the base level where collisions occur. Successively, the maximum responses occur at the 1-0 interface, while the influence of the excitation angle persists for the upper floors.

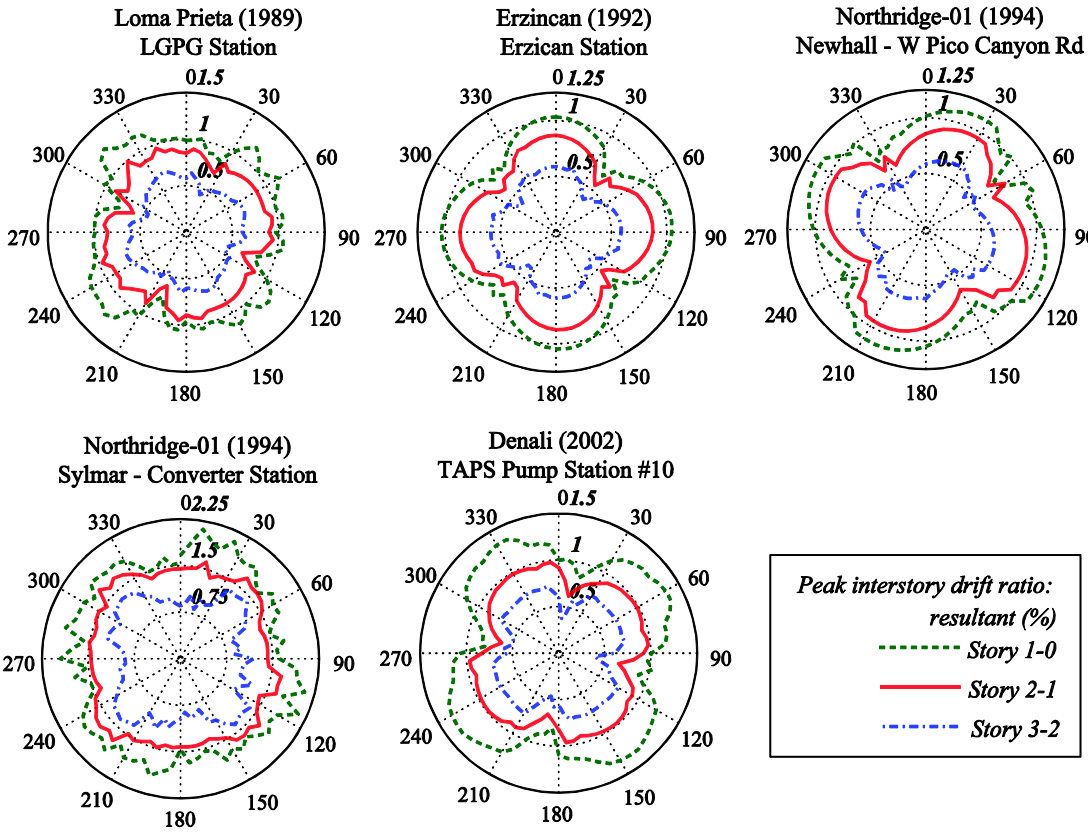

Fig. 6 – Polar plots of the peak resultant interstory drift ratios at each floor of the corner column A_1 for varying seismic incidence angles, while considering a seismic gap of 20 cm.

3.3 Influence of mass eccentricity

As torsional effects can potentially occur even in absolutely symmetric structures due to mass eccentricities, modern codes for earthquake resistant building design require consideration of the so-called accidental design eccentricity. Fig. 7 provides the envelope of the peak interstory deflection resultant ratio among the 4 corner columns both without and with unidirectional (blue dashed line) as well as bidirectional (red dashed line) mass eccentricity of 10% of the floor plan dimension, considering a seismic gap of 20 cm and the incidence angle of the imposed excitation varying from 0° to 360°.

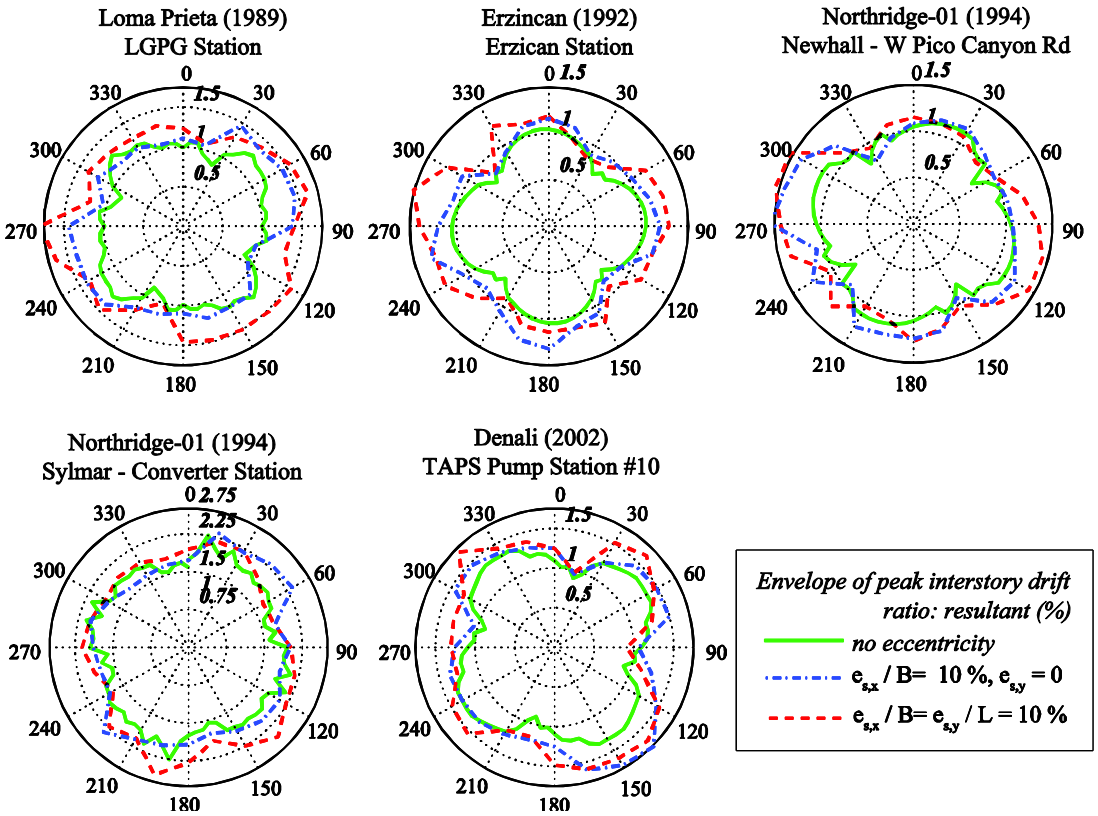

Fig. 7 – Plot of the envelope of the peak interstory deflection resultant ratio among corner columns with/without accidental mass eccentricity at the superstructure, assuming an available seismic gap between the simulated structure and the retaining walls at 20 cm.

In general, the peak seismic response amplification tends to increase for buildings with such irregularities, although the incidence angle continues to be the dominant factor influencing the overall response. The effect of the angle of incidence on the peak seismic response is significantly different in symmetrical and unsymmetrical conditions. These investigations indicate that, in general, structural elements in asymmetric-plan systems, such as those examined due to bidirectional mass eccentricities, are likely to experience higher interstory drifts, than elements of symmetric structures (no eccentricity).

Therefore, the process of determining the critical incidence angle is more complex when considering accidental mass eccentricities. Since it is not possible to know a priori the incidence direction that may generate the highest seismic response, it is necessary to perform numerous analyses for different incidence angles. Different models should also be used to explicitly evaluate various locations of accidental mass eccentricities, as well as different angles of incidence. The findings of this investigation suggest that in order to take into account properly such effects, time-history analyses should be performed to identify “the worst-case scenario”. Alternatively, if an approach that does not explicitly account for accidental mass eccentricity is employed, appropriate safety factors should be devised and used.

3.4. Effect of adjacent structural arrangement

Given that the seismic response of base-isolated structures subjected to strong excitations depends on the excitation characteristics, the sensitivity of the calculated nonlinear dynamic response of the 3-story BIB during pounding against adjacent fixed-supported buildings or/and the surrounding moat wall is examined next. It should be noted that the neighboring buildings are simulated as linear MDOF systems, possessing the same superstructures’ characteristics as the BIB and located in the same distance as the moat wall. For simplicity, it is assumed that the floor-slabs of the neighboring buildings are located at the same levels, leading to potential slab-to-slab poundings and neglecting any slab-to-column interactions.

The peak seismic responses of the examined BIB are discussed next, assuming an available seismic gap between the simulated structure and the adjacent structures, in the east direction, of 20 cm. Fig. 8 presents the envelope of the peak interstory drift ratios (resultant) at each floor of the BIB among all corner columns during poundings with the adjacent structures, for various orientations of the ground motions. In general, the variation of the response ratios, seems to be influenced by the earthquake excitation's characteristics (frequency content and directionality), as these plots show that peak interstory deflection ratios can vary by a factor of 2.5 over the possible angles of incidence, at least for the gap size of 20 cm that is considered herein.

It can be observed that the peak interstory deflection ratios for the case of the BIB pounding against only with the surrounding moat wall are, in general, higher than for the case of buildings in series with pounding against the adjacent conventionally fixed-supported buildings. Although, the computed peak seismic response that is provided in Fig. 8 suggests that the number of floors of the adjacent buildings can significantly affect the overall dynamic response of the BIB, one cannot generalize the severity of the influence based on the number of floors. What one can generalize is that the critical response is polarized at a specific direction irrespective of the number of stories of surrounding buildings.

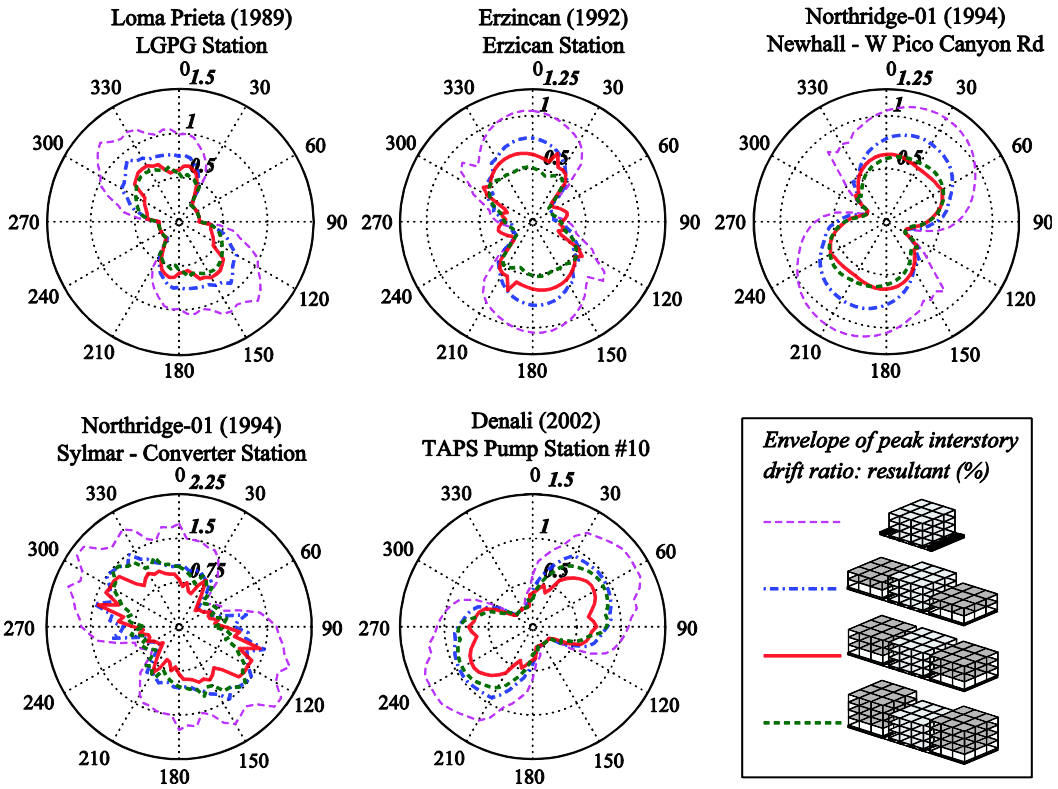

Fig. 8 – Envelope of peak resultant interstory drifts ratio of the BIB during poundings, in terms of the angle of incidence, considering a gap size of 20 cm and various configurations of the adjacent conventionally fixed-supported structures, located on the east side of the BIB.

4. Major Findings

Numerical simulations of a BIB have been conducted under five strong earthquake excitations in order to investigate the influence of the width of the available seismic gap on the peak interstory deflections during potential poundings. The numerical simulations demonstrate that higher modes of vibration are excided during poundings, increasing the interstory deflections, instead of retaining an almost rigid-body motion of the superstructure, which is aimed with seismic isolation.

Parametric studies that simulate earthquake-induced pounding of the BIB under consideration have been conducted in 3D in order to investigate the influence of the incidence angle, the spatial configurations of the adjacent structures and accidental mass eccentricities of the BIB, on its peak seismic response in terms of interstory drifts. The computed results of the performed simulations show that the impacts are particularly unfavorable for the BIB since they significantly amplify interstory deflections of the superstructure of the BIB, which could lead to structural and non-structural damage. Furthermore, they reveal that the detrimental effects of pounding may become more severe for certain values of the incidence angle which, in general, are different from the major construction axes, at 0^o and 90^o, the most commonly employed directions in practice while performing time-history analysis. The incidence angle along which the amplification of the superstructure's response due to pounding with the adjacent structures obtains its maximum value, in case of pounding only to the surrounding moat wall, generally coincides with the angle along which the peak unobstructed relative displacement at the isolation level occurs. On the other hand, one can conclude that the process of determining the critical incidence angle is more complex when considering adjacent multistory structures and, since generalizations cannot be made, numerical simulations should be performed for each specific case in order to more reliably investigate the possibility of structural pounding and the corresponding peak seismic response.

5. References

[1] Skinner RI, Robinson WH, McVerry GH (1993): An introduction to seismic isolation. West Sussex, UK: John Wiley & Sons Ltd.

[2] Naeim F, Kelly JM (1999): Design of seismic isolated structures: From theory to practice. Hoboken NJ, USA: John Wiley & Sons Inc.

[3] Komodromos P (2000): Seismic Isolation for Earthquake Resistant Structures. Southampton: WIT Press.

[4] Higashino M, Okamoto S (2006): Response Control and Seismic Isolation of Buildings. Oxon, UK.

[5] Polycarpou PC, Komodromos P (2010): On poundings of a seismically isolated building with adjacent structures during strong earthquakes. *Earthquake Engineering and Structural Dynamics*, **39**(8), 1397–1951.

[6] Mahmoud S, Jankowski R (2010): Pounding-involved response of isolated and non-isolated buildings under earthquake excitation. *Earthquakes and Structures*, **1**(3), 231–252.

[7] Polycarpou PC, Komodromos P (2011): Numerical investigation of potential mitigation measures for poundings of seismically isolated buildings. *Earthquakes and Structures*, **2**(1), 1–24.

[8] Masroor A, Mosqueda G (2013): Seismic response of base isolated buildings considering pounding to moat walls: MCEER-13-0003.

[9] Anagnostopoulos SA (1988): Pounding of buildings in series during earthquakes. *Earthquake Engineering and Structural Dynamics*, **16**, 443–456.

[10] Anagnostopoulos SA, Spiliopoulos K V. (1992): An investigation of earthquake induced pounding between adjacent buildings. *Earthquake Engineering and Structural Dynamics*, **21**(4), 289–302.

[11] Filiatrault A, Wagner P, Cherry S (1995): Analytical prediction of experimental building pounding. *Earthquake Engineering and Structural Dynamics*, **24**(8), 1131–1154.

[12] Matsagar VA, Jangid RS (2003): Seismic response of base-isolated structures during impact with adjacent structures. *Engineering Structures*, **25**(10), 1311–1323.

[13] Komodromos P, Polycarpou PC, Papaloizou L, Phocas MC (2007): Response of seismically isolated buildings considering poundings. *Earthquake Engineering and Structural Dynamics*, **36**(12), 1605–1622.

[14] Komodromos P (2008): Simulation of the earthquake-induced pounding of seismically isolated buildings. *Earthquake Engineering and Structural Dynamics*, **86**(7–8), 618–626.

[15] Dimitrakopoulos E, Makris N, Kappos AJ (2009): Dimensional analysis of the earthquake-induced pounding between adjacent structures. *Earthquake Engineering and Structural Dynamics*, **38**, 867–886.

[16] Ye K, Li L, Zhu H (2009): A modified Kelvin impact model for pounding simulation of base-isolated building

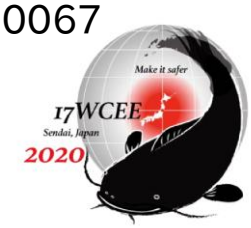

with adjacent structures. *Earthquake Engineering and Engineering Vibration*, **8**(3), 433–446.

[17] Mavronicola E, Polycarpou P, Papaloizou L, Komodromos P (2015): Computer-aided investigation of special issues of the response of seismically isolated buildings. *International Journal of Computational Methods and Experimental Measurements*, **3**(1), 21–32.

[18] Jankowski R, Mahmoud S (2015): Earthquake-Induced Structural Pounding. Springer International Publishing.

[19] Mavronicola EA, Polycarpou PC, Komodromos P (2016): Effect of Planar Impact Modeling on the Pounding Response of Base-Isolated Buildings. *Frontiers in Built Environment*, **2**, 11. Frontiers.

[20] Bao Y, Becker TC (2018): Inelastic response of base-isolated structures subjected to impact. *Engineering Structures*, **171**, 86–93.

[21] Matsagar VA, Jangid RSS (2010): Impact Response of Torsionally Coupled Base-isolated Structures. *Journal of Vibration and Control*, **16**(11), 1623–1649.

[22] Sato E, Furukawa S, Kakehi A, Nakashima M (2011): Full-scale shaking table test for examination of safety and functionality of base-isolated medical facilities. *Earthquake Engineering and Structural Dynamics*, **40**(13), 1435–1453.

[23] Pant DR, Wijeyewickrema AC (2012): Structural performance of a base-isolated reinforced concrete building subjected to seismic pounding. *Earthquake Engineering and Structural Dynamics*, **41**(12), 1709–1716.

[24] Masroor A, Mosqueda G (2012): Experimental simulation of base-isolated buildings pounding against moat wall and effects on superstructure response. *Earthquake Engineering and Structural Dynamics*, **41**(14), 2093–2109.

[25] Varnava V, Komodromos P (2013): Assessing the effect of inherent nonlinearities in the analysis and design of a low-rise base isolated steel building. *Earthquakes and Structures*, **5**(5), 499–526.

[26] Masroor A, Mosqueda G (2013): Impact model for simulation of base isolated buildings impacting flexible moat walls. *Earthquake Engineering and Structural Dynamics*, **42**(3), 357–376.

[27] Pant DR, Wijeyewickrema AC (2014): Performance of base-isolated reinforced concrete buildings under bidirectional seismic excitation considering pounding with retaining walls including friction effects. *Earthquake Engineering and Structural Dynamics*, **43**(10), 1521–1541.

[28] Polycarpou PC, Papaloizou L, Komodromos P (2014): An efficient methodology for simulating earthquake-induced 3D pounding of buildings. *Earthquake Engineering and Structural Dynamics*, **43**(7), 985–1003.

[29] Mavronicola EA, Polycarpou PC, Komodromos P (2017): Spatial seismic modeling of base-isolated buildings pounding against moat walls: effects of ground motion directionality and mass eccentricity. *Earthquake Engineering and Structural Dynamics*, **46**(7), 1161–1179.

[30] PEER Pacific Earthquake Engineering Research Center (2011): Ground motion database. Retrieved November 23, 2011, from http://peer.berkeley.edu/peer_ground_motion_database

[31] Wen Y-K (1976): Method for random vibration of hysteretic systems. *Journal of the Engineering Mechanics Division*, **102**(2), 249–263.

[32] Park YJ, Wen Y-K, Ang A (1986): Random vibration of hysteretic systems under bi-directional ground motions. *Earthquake Engineering and Structural Dynamics*, **14**(4), 543–557.

[33] Jankowski R (2005): Non-linear viscoelastic modelling of earthquake-induced structural pounding. *Earthquake Engineering and Structural Dynamics*, **34**(6), 595–611.

[34] Anagnostopoulos SA, Karamaneas CE (2008): Use of collision shear walls to minimize seismic separation and to protect adjacent buildings from collapse due to earthquake-induced pounding. *Earthquake Engineering and Structural Dynamics*, **37**(12), 1371–1388.

[35] Athanatopoulou AM (2005): Critical orientation of three correlated seismic components. *Engineering Structures*, **27**(2), 301–312.

[36] Polycarpou PC, Papaloizou L, Komodromos P, Charmpis DC (2015): Effect of the seismic excitation angle on the dynamic response of adjacent buildings during pounding. *Earthquakes and Structures*, **8**(5), 1127–1146.

